

# Free Vibration Analysis of Smart FGM Plates

F.Ebrahimi, A.Rastgo

**Abstract**—Analytical investigation of the free vibration behavior of circular functionally graded (FG) plates integrated with two uniformly distributed actuator layers made of piezoelectric (PZT4) material on the top and bottom surfaces of the circular FG plate based on the classical plate theory (CPT) is presented in this paper. The material properties of the functionally graded substrate plate are assumed to be graded in the thickness direction according to the power-law distribution in terms of the volume fractions of the constituents and the distribution of electric potential field along the thickness direction of piezoelectric layers is simulated by a quadratic function. The differential equations of motion are solved analytically for clamped edge boundary condition of the plate. The detailed mathematical derivations are presented and Numerical investigations are performed for FG plates with two surface-bonded piezoelectric layers. Emphasis is placed on investigating the effect of varying the gradient index of FG plate on the free vibration characteristics of the structure. The results are verified by those obtained from three-dimensional finite element analyses.

**Keywords**—Circular plate, CPT, Functionally graded, Piezoelectric.

## 1. INTRODUCTION

A NEW class of materials known as ‘functionally graded materials’ (FGMs) has emerged recently, in which the material properties are graded but continuous particularly along the thickness direction. In an effort to develop the super heat resistant materials, Koizumi [1] first proposed the concept of FGM. These materials are microscopically heterogeneous and are typically made from isotropic components, such as metals and ceramics.

In the quest for developing lightweight high performing flexible structures, a concept emerged to develop structures with self-controlling and self-monitoring capabilities. Expediently, these capabilities of a structure were achieved by exploiting the converse and direct piezoelectric effects of the piezoelectric materials as distributed actuators or sensors, which are mounted or embedded in the structure [2, 3]. Such structures having built-in mechanisms are customarily known as ‘smart structures’. The concept of developing smart structures has been extensively used for active control of flexible structures during the past decade [4].

Recently considerable interest has also been focused on

investigating the performance of FG plates integrated with piezoelectric actuators. For example, Ootao and Tanigawa [5] theoretically investigated the simply supported FG plate integrated with a piezoelectric plate subjected to transient thermal loading. A 3-D solution for FG plates coupled with a piezoelectric actuator layer was proposed by Reddy and Cheng [6] using transfer matrix and asymptotic expansion techniques. Wang and Noda [7] analyzed a smart FG composite structure composed of a layer of metal, a layer of piezoelectric and a FG layer in between, while in [8] a finite element model was developed for studying the shape and vibration control of FG plates integrated with piezoelectric sensors and actuators. Yang et al. [9] investigated the nonlinear thermo-electro-mechanical bending response of FG rectangular plates covered with monolithic piezoelectric actuator layers; most recently, Huang and Shen [10] investigated the dynamics of a FG plate coupled with two monolithic piezoelectric layers undergoing nonlinear vibrations in thermal environments. All the aforementioned studies focused on the rectangular-shaped plate structures.

The present work attempts to solve the problem of providing analytical solution for free vibration of thin circular FG plates with two full size surface-bonded piezoelectric layers on the top and the bottom of the FG plate. The formulations are based on CPT. A consistent formulation that satisfies the Maxwell static electricity equation is presented so that the full coupling effect of the piezoelectric layer on the dynamic characteristics of the circular FGM plate can be estimated based on the free vibration results. The physical and mechanical properties of the FG substrate plate are assumed to be graded continuously in the thickness direction according to the power-law distribution in terms of the volume fractions of the constituents. The differential equations of motion are solved analytically for clamped edge boundary condition of the plate. By using of some mathematical techniques these differential equations are transformed to a sixth order ordinary differential equation and finally by implementing the operator decomposition method on this equation, three Bessel types of equations are obtained which can easily be solved for the plate deflection and the potential function. The detailed mathematical derivations are presented. In Numerical investigations, the emphasis is placed on investigating the effect of varying the gradient index of FG plate on the free vibration characteristics of the structure. The results are verified by those obtained from 3D finite element analyses.

Manuscript received September 13, 2007.

F. Ebrahimi is a Ph.D student in the Faculty of Mechanical Engineering at the University of Tehran, Tehran, Iran (corresponding author to provide phone: +98 21 88005677; fax: +98 21 88013029; e-mail: febrahimi@ut.ac.ir).

A. Rastgoo is a professor with the Faculty of Mechanical Engineering at the University of Tehran, Tehran, Iran (e-mail: arastgo@ut.ac.ir).

## II. FUNCTIONALLY GRADED MATERIALS

In a FG material made of ceramic and metal mixture, if the volume fraction of the ceramic part is represented by  $V_c$  and the metallic part by  $V_m$ , we have;

$$V_m + V_c = 1 \quad (1)$$

Based on the power law distribution [11], the variation of  $V_c$  vs. thickness coordinate ( $z$ ) placed at the middle of thickness, can be expressed as;

$$V_c = (z/2h_f + 1/2)^g, \quad g \geq 0 \quad (2)$$

We assume that the inhomogeneous material properties, such as the modulus of elasticity  $E$  and the density  $\rho$  change in the thickness direction  $z$  based on Voigt's rule over the whole range of the volume fraction [12]; while Poisson's ratio  $\nu$  is assumed to be constant in the thickness direction [13] as;

$$E(z) = (E_c - E_m)V_c(z) + E_m \quad (3a)$$

$$\rho(z) = (\rho_c - \rho_m)V_c(z) + \rho_m \quad (3b)$$

where subscripts  $m$  and  $c$  refer to the metal and ceramic constituents, respectively. After substituting  $V_c$  from Eq. (2) into Eqs. (3), material properties of the FGM plate are determined in the power law form which are the same as those proposed by Reddy et al. [11] i.e.;

$$E(z) = (E_c - E_m)(z/2h_f + 1/2)^g + E_m \quad (4a)$$

$$\rho(z) = (\rho_c - \rho_m)(z/2h_f + 1/2)^g + \rho_m \quad (4b)$$

$$\nu(z) = \nu \quad (4c)$$

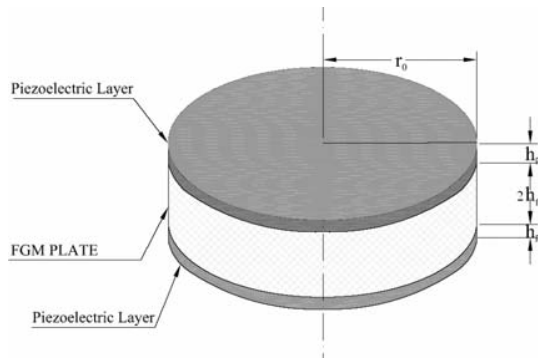


Fig. 1 Piezoelectric Coupled FGM circular plate

## III. PIEZOELECTRIC MATERIALS

For symmetry piezoelectric materials in polar coordinate, the stress - strain - electric field intensity relations based on well-known assumptions of classical plate theory, can be written as [16];

$$\sigma_{rr}^p = \bar{C}_{11}^E \varepsilon_{rr} + \bar{C}_{12}^E \varepsilon_{\theta\theta} - \bar{e}_{31}^E E_z \quad (5)$$

$$\sigma_{\theta\theta}^p = \bar{C}_{12}^E \varepsilon_{rr} + \bar{C}_{11}^E \varepsilon_{\theta\theta} - \bar{e}_{31}^E E_z \quad (6)$$

$$\tau_{r\theta}^p = (\bar{C}_{11}^E - \bar{C}_{12}^E) \varepsilon_{r\theta} = -z(\bar{C}_{11}^E - \bar{C}_{12}^E) \quad (7)$$

in which  $\sigma_i$ ,  $\varepsilon_k$  and  $e$  represent the stress and strain components and the permeability constant of piezoelectric material and  $E_k$  indicates the components of the electric field. and  $\bar{C}_{ij}^E$  are the components of the symmetric piezoelectric stiffness matrix and  $\bar{e}_{31}^E$  is the reduced permeability constant of piezoelectric material as [13];

$$\bar{C}_{11}^E = C_{11}^E - (C_{13}^E)^2 / C_{33}^E, \quad \bar{C}_{12}^E = C_{12}^E - (C_{13}^E)^2 / C_{33}^E$$

$$\bar{e}_{31}^E = e_{31}^E - C_{13}^E e_{33}^E / C_{33}^E$$

## IV. CONSTITUTIVE RELATIONS

The cross section of a circular FGM plate with a piezoelectric layer mounted on its surface is shown in Fig. 1. In most practical applications, the ratio of the radius to the thickness of the plate is more than ten, and the Kirchhoff assumption for thin plates is applicable, whereby the shear deformation and rotary inertia can be omitted. For such a structure, the displacement field is assumed as follows:

$$u_z = u_z(r, \theta, t) = w(r, \theta, t) \quad (8)$$

$$u_r = u_r(r, \theta, t) = -z \frac{\partial u_z}{\partial r} \quad (9)$$

$$u_\theta = u_\theta(r, \theta, t) = -z \frac{\partial u_z}{r \partial \theta} \quad (10)$$

where  $u_z$ ,  $u_r$ , and  $u_\theta$  are the displacements in the transverse  $z$ -direction, radial  $r$ -direction, and tangential  $\theta$ -direction of the plate, respectively.

It is also assumed that the poling direction of the piezoelectric material to be in the  $z$ -direction. A differential strain can be induced in case of applying external electric potential across the piezoelectric layer resulting in bending of the plate. The strain of the FGM plate and piezoelectric layer in the radial and tangential directions and the shear component are given by [14]

$$\varepsilon_{rr} = \frac{\partial u_r}{\partial r} = -z \frac{\partial^2 w}{\partial r^2} \quad (11)$$

$$\varepsilon_{\theta\theta} = \frac{\partial u_\theta}{r \partial \theta} + \frac{u_r}{r} = -z \left( \frac{\partial^2 w}{r^2 \partial \theta^2} + \frac{\partial w}{r \partial r} \right) \quad (12)$$

$$\varepsilon_{r\theta} = \frac{1}{2} \left( \frac{\partial u_r}{r \partial \theta} + \frac{\partial u_\theta}{\partial r} - \frac{u_\theta}{r} \right) \quad (13)$$

The stress components in the FGM plate in terms of strains

or component of displacement field based on the generalized Hooke's Law are [14];

$$\sigma_{rr}^f = E(z)(\epsilon_{rr} + \nu\epsilon_{\theta\theta}) / (1 - \nu^2) \tag{14}$$

$$\sigma_{\theta\theta}^f = E(z)(\epsilon_{\theta\theta} + \nu\epsilon_{rr}) / (1 - \nu^2) \tag{15}$$

$$\tau_{r\theta}^f = -\frac{zE(z)}{1 + \nu} \left( \frac{\partial^2 w}{r\partial r\partial\theta} - \frac{\partial w}{r^2\partial\theta} \right) \tag{16}$$

where the superscript *f* represents the variable in the FGM structure; Two piezoelectric layers are attached to the FG plate and intended to be used as an actuator or sensor to determine the natural frequencies of a vibrating coupled plate. There are several different models representing the input electric potential for such a piezoelectric layer. In this paper we decided to adopt the following Wang et al. electric potential function which is appropriate for free vibrations of proposed system [13];

$$\phi = \left[ 1 - \left( \frac{2z - 2h_f - h_p}{h_p} \right)^2 \right] \varphi(r, \theta, t) \tag{17}$$

where  $\varphi(r, \theta, t)$  is the electric potential on the mid-surface of the piezoelectric layer.

Based on Eq. (17), the components of electric field intensity *E* and electric flux density *D* is written as [15]:

$$D_r = \bar{\epsilon}_{11} E_r = \bar{\epsilon}_{11} \left( -\frac{\partial\phi}{\partial r} \right) \tag{18}$$

$$D_\theta = \bar{\epsilon}_{11} E_\theta = \bar{\epsilon}_{11} \left( -\frac{\partial\phi}{r\partial\theta} \right) \tag{19}$$

$$D_z = \bar{\epsilon}_{33} E_z + \bar{e}_{31} (\epsilon_{rr} + \epsilon_{\theta\theta}) \tag{20}$$

where  $\bar{\epsilon}_{11}, \bar{\epsilon}_{33}$  are the symmetric reduced dielectric constants of piezo layer and given by [17];

$$\bar{\epsilon}_{33} = \bar{\epsilon}_{33} + (e_{33}^2 / C_{33}^E) \quad , \quad \bar{\epsilon}_{11} = \bar{\epsilon}_{11} \tag{21}$$

in which  $\bar{\epsilon}_{33}, \bar{\epsilon}_{11}$  are the dielectric constants.

### V. GOVERNING EQUATIONS

In order to obtain the governing differential equation of the coupled circular plate, we begin with resultant moments components as [16];

$$M_{rr} = \int_{-h_f}^{h_f} z \sigma_{rr}^f dz + 2 \int_{h_f}^{h_f+h_p} z \sigma_{rr}^p dz \tag{22}$$

$$M_{\theta\theta} = \int_{-h_f}^{h_f} z \sigma_{\theta\theta}^f dz + 2 \int_{h_f}^{h_f+h_p} z \sigma_{\theta\theta}^p dz \tag{23}$$

$$M_{r\theta} = \int_{-h_f}^{h_f} z \tau_{r\theta}^f dz + 2 \int_{h_f}^{h_f+h_p} z \tau_{r\theta}^p dz \tag{24}$$

And the resultant shear forces are herein written as

$$q_r = \frac{\partial M_{rr}}{\partial r} + \frac{\partial M_{r\theta}}{r\partial\theta} + \frac{M_{rr} - M_{\theta\theta}}{r} \tag{25}$$

$$q_\theta = \frac{\partial M_{r\theta}}{\partial r} + \frac{\partial M_{\theta\theta}}{r\partial\theta} + \frac{2M_{r\theta}}{r} \tag{26}$$

Substituting Eqs. (11-13) in to Eqs. (14-16) and Eqs. (5-7) and substituting the results in to Eqs. (22-26) and substituting the final results into the governing equation for the Kirchhoff plate,

$$\frac{\partial q_r}{\partial r} + \frac{\partial q_\theta}{r\partial\theta} + \frac{q_r}{r} - \left( \int_{-h_f}^{h_f} \rho_f(z) \frac{\partial^2 u_z}{\partial t^2} dz + 2 \int_{h_f}^{h_f+h_p} \rho_p \frac{\partial^2 u_z}{\partial t^2} dz \right) = 0 \tag{27}$$

will result in the equation for the piezoelectric coupled circular FGM plate,

$$(D_1 + D_2) \Delta \Delta w + \frac{4}{3} h_p \bar{e}_{31} \Delta \phi + P_0 \frac{\partial^2 w}{\partial t^2} = 0 \tag{28}$$

where  $\Delta$  is the Laplace operator in polar coordinate and

$$D_1 = \int_{-h_f}^{h_f} \frac{z^2 E(z)}{1 - \nu^2} dz \quad , \quad D_2 = \frac{2}{3} h_p (3h_f^2 + 3h_f h_p + h_p^2) \bar{C}_{11}^E$$

$$\tilde{\rho}_f = \frac{1}{2h_f} \int_{-h_f}^{h_f} \rho_f(z) dz \quad , \quad P_0 = 2(\tilde{\rho}_f h_f + \tilde{\rho}_p h_p)$$

where  $\rho_f$  and  $\rho_p$  are material densities of the FGM plate and piezoelectric layer, respectively.

Note that all of the electrical variables primarily must satisfy the Maxwell's equation which requires that the divergence of the electric flux density vanishes at any point within the media as [15];

$$\int_{h_f}^{h_f+h_p} \left( \frac{\partial(rD_r)}{r\partial r} + \frac{\partial D_\theta}{r\partial\theta} + \frac{\partial D_z}{\partial z} \right) dz = 0 \tag{29}$$

Now, by substituting Eqs. (18- 20) into the above equation we arrive at;

$$\frac{h_p^2 \bar{\epsilon}_{11}}{12 \bar{\epsilon}_{33}} \Delta \phi - \phi + \frac{h_p^2 \bar{e}_{31}}{8 \bar{\epsilon}_{33}} \Delta w = 0 \tag{30}$$

### VI. SOLUTIONS METHOD

Primarily we solve Eqs. (28) and (30) simultaneously by which  $\phi$  can be expressed in terms of *w* as;

$$\varphi(r, \theta, t) = -\frac{(D_1 + D_2)h_p \bar{\Xi}_{11}}{16\bar{e}_{31}\bar{\Xi}_{33}} \Delta \Delta w + \frac{h_p^2 \bar{e}_{31}}{8\bar{\Xi}_{33}} \Delta w - \frac{h_p (\bar{\rho}_f h_f + \rho_p h_p) \bar{\Xi}_{11}}{8\bar{e}_{31}\bar{\Xi}_{33}} \frac{\partial^2 w}{\partial t^2} \quad (31)$$

Applying the Laplacian operator to the above equation and substituting the result into equation (28) gives a decoupled sixth-order partial differential equation, namely

$$P_3 \Delta \Delta \Delta w - P_2 \Delta \Delta w + P_1 \Delta \left( \frac{\partial^2 w}{\partial t^2} \right) - P_0 \frac{\partial^2 w}{\partial t^2} = 0 \quad (32)$$

where

$$P_1 = h_p^2 \bar{\Xi}_{11} P_0 / 12 \bar{\Xi}_{33}, \quad P_2 = D_1 + D_2 + h_p^3 \bar{e}_{31}^2 / 6 \bar{\Xi}_{33} \\ P_3 = (D_1 + D_2) h_p^2 \bar{\Xi}_{11} / 12 \bar{\Xi}_{33} \quad (33)$$

To solve Eq. (34) for  $w$ , we first assume that;

$$w(r, \theta, t) = w_1(r) e^{i(m\theta - \omega t)} \quad (34)$$

where  $w_1(r)$  is the displacement amplitude in the  $z$  - direction as a function of radial displacement only;  $\omega$  is the natural angular frequency of the compound plate; and  $m$  is the wave number in the circumferential direction. Rewriting Eq. (32) in terms of  $w_1(r)$  and using Eq. (34), after canceling the exponential term one would get;

$$P_3 \bar{\Delta} \bar{\Delta} \bar{\Delta} w_1 - P_2 \bar{\Delta} \bar{\Delta} w_1 - \omega^2 P_1 \bar{\Delta} w_1 + \omega^2 P_0 w_1 = 0 \quad (35)$$

where  $\bar{\Delta} = d^2/dr^2 + d/r dr - m^2/r^2$ .

Eq. (35) can be solved by the method of decomposition operator and noting that the  $w_1$  is non-singular at the center of the plate its general solution yields to

$$w_1 = \sum_{n=1}^3 A_{nm} Z_{nm}(\alpha_n r) \quad (36)$$

where

$$\alpha_1 = \sqrt{|x_1|}, \alpha_2 = \sqrt{|x_2|}, \alpha_3 = \sqrt{|x_3|} \quad (37)$$

in which  $x_1, x_2$  and  $x_3$  are the roots of the following cubic characteristic equation,

$$P_3 x^3 - P_2 x^2 - \omega^2 P_1 x + \omega^2 P_0 = 0 \quad (38)$$

and

$$Z_{im}(\alpha_i r) = Z_{im}(\alpha_i, r) = \begin{cases} J_m(\alpha_i r) & , x_i < 0 \\ I_m(\alpha_i r) & , x_i > 0 \end{cases} \quad (39)$$

here  $i=(1,2,3)$  and  $J_m(\alpha_i r), I_m(\alpha_i r)$  are the first type and the

modified first type Bessel function ,both of them of the order of  $m$ . In order to obtain appropriate solution for  $\varphi(r, \theta, t)$ , we assume;

$$\varphi(r, \theta, t) = \varphi_1(r) e^{i(m\theta - \omega t)} \quad (40)$$

then substituting Eq. (36) in to Eq. (31) we arrive to the following relation for  $\varphi(r, \theta, t)$  ;

$$\varphi_1(r) = [16\bar{e}_{31}\bar{\Xi}_{33}]^{-1} \sum_{n=1}^3 [A_{nm} h_p (2s_n \alpha_n^2 h_p \bar{e}_{31}^2 - (D_1 + D_2) \alpha_n^4 \bar{\Xi}_{11} + P_0 \omega^2 \bar{\Xi}_{11})] \times Z_{nm}(\alpha_n r) \quad (41)$$

### VII. CASE STUDIES, RESULTS AND DISCUSSIONS

We will solve above the relations in this section; the material parameters and geometries are listed in Table I.

TABLE I  
MATERIAL PROPERTIES AND GEOMETRIC SIZE OF THE PIEZOELECTRIC COUPLED FGM PLATE [13, 17]

FGM Plate:	$E_c = 205 \text{ GPa}$	$\rho_c = 8900 \text{ (kg/ m}^3\text{)}$
	$E_m = 200 \text{ GPa}$	$\rho_m = 7800$
PZT4:	$C_{11}^E = 132$	$C_{33}^E = 115$
	$C_{55}^E = 26 \text{ GPa}$	$C_{12}^E = 71$
	$e_{31} = -4.1 \text{ (C/m}^2\text{)}$	$e_{15} = 10.5$
	$\bar{\Xi}_{11} = 7.124 \text{ (nF/m)}$	$\bar{\Xi}_{33} = 5.841$
		$\rho_p = 7500 \text{ (kg/ m}^3\text{)}$
Geometry(mm):	$r_0 = 600$	$h_i = 2, h_p = 10$

#### A. Clamped circular Piezo-coupled FGM plate

The boundary condition is given by

$$w_1 = dw_1/dr = d\varphi_1/dr = 0 \quad \text{at } (r = r_0) \quad (42)$$

and the characteristic equation is

$$\begin{vmatrix} c_{11} & c_{12} & c_{13} \\ c_{21} & c_{22} & c_{23} \\ c_{31} & c_{32} & c_{33} \end{vmatrix} = 0 \quad (43)$$

$$c_{1i} = Z_{im}(\alpha_i r_0)$$

$$c_{2i} = \alpha_i r_0 Z'_{im}(\alpha_i r_0)$$

$$c_{3i} = \left( \frac{h_p^2 r_0 s_i \alpha_i^3}{8} - \frac{(D_1 + D_2) h_p r_0 \alpha_i^5 \bar{\Xi}_{11}}{16 \bar{e}_{31}^2} + \frac{(D_1 + D_2) h_p \alpha_i \lambda^4 \bar{\Xi}_{11}}{16 \bar{e}_{31}^2 r_0^3} \right) Z'_{im}(\alpha_i r_0) \quad (44)$$

$$\lambda = r_0 \left[ \frac{2(\tilde{\rho}_f h_f + \rho_p h_p) \omega^2}{D_1 + D_2} \right]^{\frac{1}{4}} \tag{45}$$

$$\omega = \frac{\lambda^2}{r_0^2} \sqrt{\frac{D_1 + D_2}{2(\tilde{\rho}_f h_f + \rho_p h_p)}} \tag{46}$$

in which the  $(\cdot)'$  symbol indicates the derivative with respect to  $r$  and  $\lambda$  is the nondimensional angular natural frequency.

TABLE II  
FIRST THREE RESONANCE FREQUENCIES (HZ) OF FGM PLATE

Power Index	Mode no.	FGM plate			
g	m	Present Method	Present (FEM)	Error (%)	Wang et al. [13]
0	0	138.42	139.27	0.61	138.48
	1	288.05	289.70	0.57	288.20
	2	472.55	473.45	0.19	472.79
1	0	134.63	135.43	0.59	-
	1	280.17	281.78	0.57	-
	2	459.62	460.45	0.18	-
3	0	132.70	133.63	0.69	-
	1	276.19	278.04	0.67	-
	2	453.09	454.34	0.28	-
5	0	132.12	133.06	0.70	-
	1	274.96	276.85	0.68	-
	2	451.06	452.39	0.29	-
7	0	131.85	132.78	0.70	-
	1	274.39	276.25	0.67	-
	2	450.13	451.46	0.29	-
9	0	131.69	132.70	0.76	-
	1	274.07	276.09	0.73	-
	2	449.60	450.84	0.28	-
10	0	131.64	132.55	0.68	-
	1	273.96	275.79	0.67	-
	2	449.42	450.66	0.28	-

After calculating  $\omega$  from Eq. (43) and using Eqs. (36, 42) we find the mode shape for  $w_l$  as;

$$w_1(r) = A_{3m} \times \left[ \left( \frac{\alpha_3 Z_{2m}(\alpha_2 r_0) Z'_{3m}(\alpha_3 r_0) - \alpha_2 Z_{3m}(\alpha_3 r_0) Z'_{2m}(\alpha_2 r_0)}{\alpha_2 Z_{1m}(\alpha_1 r_0) Z'_{2m}(\alpha_2 r_0) - \alpha_1 Z_{2m}(\alpha_2 r_0) Z'_{1m}(\alpha_1 r_0)} \right) \times Z_{1m}(\alpha_1 r) + \left( \frac{\alpha_1 Z_{3m}(\alpha_3 r_0) Z'_{1m}(\alpha_1 r_0) - \alpha_3 Z_{1m}(\alpha_1 r_0) Z'_{3m}(\alpha_3 r_0)}{\alpha_2 Z_{1m}(\alpha_1 r_0) Z'_{2m}(\alpha_2 r_0) - \alpha_1 Z_{2m}(\alpha_2 r_0) Z'_{1m}(\alpha_1 r_0)} \right) \times Z_{2m}(\alpha_2 r) + Z_{3m}(\alpha_3 r) \right] \tag{47}$$

And moreover, by using Eqs. (36, 41, 42) we have the electric potential as;

$$\hat{\phi}(r) = A_{3m} \times \left[ \left( \frac{\alpha_3 Z_{2m}(\alpha_2 r_0) Z'_{3m}(\alpha_3 r_0) - \alpha_2 Z_{3m}(\alpha_3 r_0) Z'_{2m}(\alpha_2 r_0)}{\alpha_2 Z_{1m}(\alpha_1 r_0) Z'_{2m}(\alpha_2 r_0) - \alpha_1 Z_{2m}(\alpha_2 r_0) Z'_{1m}(\alpha_1 r_0)} \right) \times Z_{1m}(\alpha_1 r) \times \left[ h_p (2s_1 \alpha_1^2 h_p \bar{e}_{31}^2 - (D_1 + D_2) \alpha_1^4 \bar{\Xi}_{11} + P_0 \omega^2 \bar{\Xi}_{11}) \right] \left[ 16 \bar{e}_{31} \bar{\Xi}_{33} \right]^{-1} \right. \tag{48}$$

$$+ \left( \frac{\alpha_1 Z_{3m}(\alpha_3 r_0) Z'_{1m}(\alpha_1 r_0) - \alpha_3 Z_{1m}(\alpha_1 r_0) Z'_{3m}(\alpha_3 r_0)}{\alpha_2 Z_{1m}(\alpha_1 r_0) Z'_{2m}(\alpha_2 r_0) - \alpha_1 Z_{2m}(\alpha_2 r_0) Z'_{1m}(\alpha_1 r_0)} \right) \times Z_{2m}(\alpha_2 r) \times \left[ h_p (2s_2 \alpha_2^2 h_p \bar{e}_{31}^2 - (D_1 + D_2) \alpha_2^4 \bar{\Xi}_{11} + P_0 \omega^2 \bar{\Xi}_{11}) \right] \left[ 16 \bar{e}_{31} \bar{\Xi}_{33} \right]^{-1} + \left[ h_p (2s_3 \alpha_3^2 h_p \bar{e}_{31}^2 - (D_1 + D_2) \alpha_3^4 \bar{\Xi}_{11} + P_0 \omega^2 \bar{\Xi}_{11}) \right] \left[ 16 \bar{e}_{31} \bar{\Xi}_{33} \right]^{-1} Z_{3m}(\alpha_3 r) \right]$$

In order to validate the obtained results, we compared our results with those given in the literature [7,9,10].

Further as there were no published results for the compound piezoelectric FGM plate, we verify the validity of obtained results with those of FEM results. Our FEM model for piezo-FG plate comprises: a 3D 8-noded solid element with: number of total nodes 26950, number of total element 24276, 3 DOF per node in the host plate element and 6 DOF per node in the piezoelectric element. Tables II and III shows the numerical results of our method compared with other references and techniques.

TABLE III  
FIRST THREE RESONANCE FREQUENCIES (HZ) FOR PIEZO-COUPLED FGM PLATE FOR VARIOUS VALUES OF POWER INDEX

Power Index	Mode no.	Coupled Piezo-FGM plate			
		Present Method	Present (FEM)	Error (%)	Wang et al. [13]
0	0	143.63	144.69	0.73	143.71
	1	298.92	300.49	0.52	299.07
	2	490.37	492.62	0.46	490.62
1	0	140.26	142.22	1.38	-
	1	291.89	295.82	1.33	-
	2	478.84	482.09	0.67	-
3	0	138.54	140.60	1.46	-
	1	288.33	292.47	1.42	-
	2	472.99	476.61	0.76	-
5	0	138.01	140.07	1.47	-
	1	287.21	291.39	1.43	-
	2	471.16	474.81	0.77	-
7	0	137.76	139.82	1.47	-
	1	286.69	290.83	1.43	-
	2	470.30	473.95	0.77	-
9	0	137.62	139.73	1.51	-
	1	286.40	290.54	1.43	-
	2	469.83	473.16	0.70	-
10	0	137.57	139.61	1.46	-
	1	286.30	290.41	1.42	-
	2	469.66	473.26	0.76	-

As one can see from Table II, the obtained results from the analytical method when  $g=0$  (isotropic steel plate) corresponds closely with the results of [7-9] and FEM solution. As it is seen in these tables the maximum estimated error of our solution with FEM is about 1.51%.

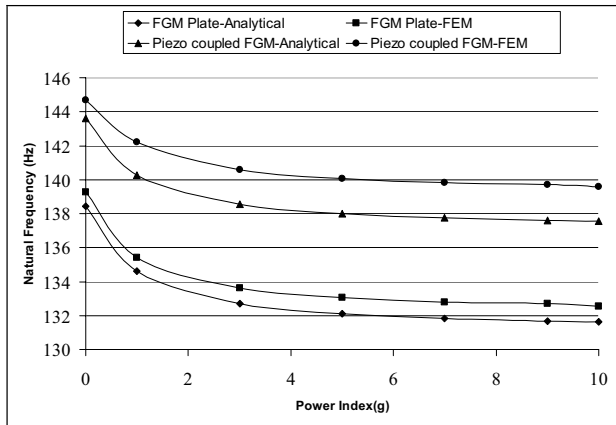


Fig. 2. Effect of power index on the natural frequencies (first mode)

A close inspection of results listed in Tables II and III indicates that the amount of error between analytical and FEM results for the natural frequencies in FGM plate alone in the all vibration modes and for all values of  $g$  are less than the similar results for the compound plate.

The obtained results in Table III indicate that by increasing the value of  $g$ , the frequency of system decreases in all different vibrational modes. Moreover, this decreasing trend of frequency for smaller values of  $g$  is more pronounced, for example by increasing value of  $g$  from 1 to 3 (~200%) the frequency of the first mode for the compound plate decreases by 1.23% but by increasing  $g$  from 3 to 9 (~ 200%) of the same plate and for the same mode, the frequency decreases by 0.66%. In order to see better the effect of  $g$  variations on the natural frequencies of the different plates, Fig. 2 and Fig. 3 also illustrate these variations for the first and third mode shapes.

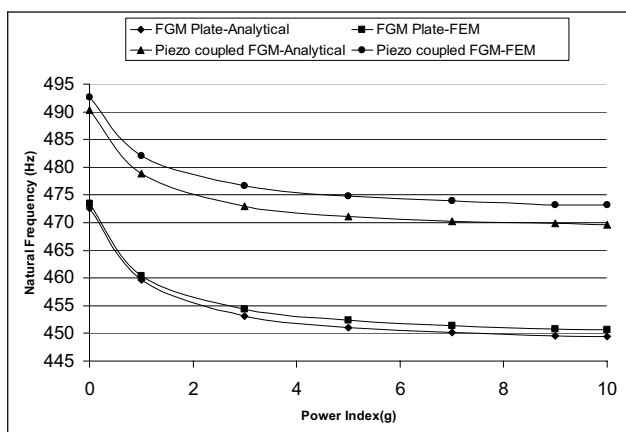


Fig. 3 Effect of power index on the natural frequencies (third mode)

As it is seen from Figs. 2 and Fig. 3, the behavior of the system follows the same trend in all different cases, i.e. the natural frequencies of the system decrease by increasing of  $g$  and stabilizes for  $g$  values greater than 7. In fact for  $g \gg 1$  the FGM plate becomes a ceramic plate and the compound plate

transforms to a laminated plate with ceramic core as a host plate.

## VIII. CONCLUSION

In this paper free vibration of a FGM plus piezoelectric laminated circular plate based on CPT is investigated. The properties of FG material changes according to the Reddy's model in direction of thickness of the plate and distribution of electric potential in the piezoelectric layers follows a quadratic function in short circuited form. The validity of the obtained results was done by crossed checking with other references as well as by obtained results from FEM solutions. It is further shown that for vibrating circular compound plates with specified dimensions, one can select a specific piezo-FGM plate which can fulfill the designated natural frequency and indeed this subject has many industrial applications.

## REFERENCES

- [1] M. Koizumi, concept of FGM, *Ceram. Trans.*, 34, 1993, 3–10.
- [2] T. Bailey & J.E. Hubbard, Distributed piezoelectric polymer active vibration control of a cantilever beam, *J. Guidance, Control Dyn.*, 8, 1985, 605–11.
- [3] S. E. Millerand & J.E. Hubbard, Observability of a Bernoulli–Euler beam using PVF2 as a distributed sensor, *MIT Draper Laboratory Report*, 1987.
- [4] F. Peng, A. Ng & Y.R. Hu, Actuator placement optimization and adaptive vibration control of plate smart structures, *J. Intell. Mater. Syst. Struct.*, 16, 2005, 263–71.
- [5] Y. Ootao & Y. Tanigawa, Three-dimensional transient piezo-thermoelasticity in functionally graded rectangular plate bonded to a piezoelectric plate, *Int. J. Solids Struct.*, 200, 37, 4377–401.
- [6] J.N. Reddy & Z.Q. Cheng, Three-dimensional solutions of smart functionally graded plates, *ASME J. Appl. Mech.*, 68, 2001, 234–41.
- [7] B.L. Wang & N. Noda, Design of smart functionally graded thermo-piezoelectric composite structure *Smart Mater. Struct.*, 10, 2001, 189–93.
- [8] X.Q. He, T.Y. Ng, S. Sivashanker & K.M. Liew, Active control of FGM plates with integrated piezoelectric sensors and actuators, *Int. J. Solids Struct.*, 38, 2001, 1641–55.
- [9] J. Yang, S. Kitipornchai & K.M. Liew, Non-linear analysis of thermo-electro-mechanical behavior of shear deformable FGM plates with piezoelectric actuators, *Int. J. Numer. Methods Eng.*, 59, 2004 1605–32.
- [10] X.L. Huang & H.S. Shen, Vibration and dynamic response of functionally graded plates with piezoelectric actuators in thermal environments, *J. Sound Vib.*, 289, 2006, 25–53.
- [11] J.N. Reddy & G.N. Praveen, Nonlinear transient thermoelastic analysis of functionally graded ceramic-metal plate *Int. J. Solids Struct.*, 35, 1998, 4457–76.
- [12] R.C. Wetherhold & S. Wang, The use of FGM to eliminate or thermal deformation, *Composite Sci Tech*, 56, 1996, 1099–104.
- [13] Q. Wang, S.T. Quek & X. Liu, Analysis of piezoelectric coupled circular plate, *Smart Mater. Struct.*, 10, 2001, 229–39.
- [14] J.N. Reddy, *Theory and analysis of elastic plates*, Philadelphia, Taylor and Francis, 1999.
- [15] D. Halliday & R. Resnick, *Physics*, John Wiley and Sons, 1978.
- [16] D.O. Brush & B.O. Almroth, *Buckling of bars plates and shells*, New York, Mac-hill, 1975.
- [17] C.T. Loy, K.L. Lam and J.N. Reddy, “Vibration of functionally graded cylindrical shells”, *Int. J Mech Sciences*, 41, 1999, 309–24